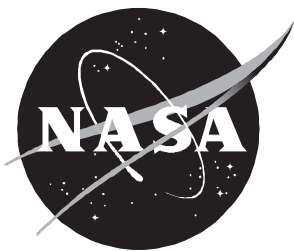


# Kinetics Model for Initiation and Promotion for Describing Tumor Prevalence From HZE Radiation

---

*Francis A. Cucinotta and John W. Wilson*



# Kinetics Model for Initiation and Promotion for Describing Tumor Prevalence From HZE Radiation

---

*Francis A. Cucinotta and John W. Wilson  
Langley Research Center • Hampton, Virginia*

This publication is available from the following sources:

NASA Center for Aerospace Information  
800 Elkridge Landing Road  
Linthicum Heights, MD 21090-2934  
(301) 621-0390

National Technical Information Service (NTIS)  
5285 Port Royal Road  
Springfield, VA 22161-2171  
(703) 487-4650

## Abstract

*A kinetics model for cellular repair and misrepair for describing multiple radiation-induced lesions (mutation-inactivation) is coupled to a two-mutation model of initiation and promotion in tissue to provide a parametric description of tumor prevalence in the Harderian gland in a mouse. Dose-response curves are described for  $\gamma$ -rays and relativistic ions. The effects of nuclear fragmentation are also considered for high-energy proton and alpha-particle exposures. The model described provides a parametric description of age-dependent cancer induction for a wide range of radiation fields. We also consider the two hypotheses that radiation acts either solely as an initiator or as both initiator and promoter and make model calculations for fractionation exposures from  $\gamma$ -rays and relativistic Fe ions. For fractionated Fe exposures, an inverse dose-rate effect is provided by a promotion hypothesis using a mutation rate for promotion typical of single-gene mutations.*

## Introduction

An understanding of the deleterious biological effects of space radiation is needed before astronauts are subjected to prolonged exposures to the high charge and energy (HZE) ion component of the galactic cosmic rays (GCR). One of the primary concerns for deep-space flight is the expected cancer risk from HZE ions. The nature of the ionizations in tissue, including the track structure, from HZE particles is very different from any other type of radiation to which humans have been exposed, and thus the expected risk is largely unknown. Although experiments with HZE exposures with cell cultures are now quite numerous (Thacker, Stretch, and Stephens 1979; Yang et al. 1985; Kronenberg and Little 1989; Kranert, Schneider, and Kiefer 1990; Lett et al. 1989), only a few experimental studies (Nelson et al. 1989; Ainsworth 1980; Burns and Albert 1980) of their mutagenic or tumorigenic potential in animal systems have been undertaken. The measurements of Fry et al. (1985) and Alpen et al. (1993 and 1994) for tumor prevalence in the Harderian gland of a mouse are the most useful of these studies because the effects on a single tumor type were considered, and dose-response curves for several ion species were studied using track-segment irradiations.

A fairly common view in cancer research is that the transformation of a single cell will result in tumor formation (Fry and Storer 1987; Land, Parada, and Weinberg 1983; Renan 1990). The discovery of oncogenes and the mechanisms for their mutation has resulted in a widely held view of carcinogenesis for many tumor types as a multistep process (Renan 1990; Mitchel and Trivedi 1993), involving

initiation, promotion, and progression. The initiation stage would include a set of mutations in the DNA of the cells produced by a carcinogen resulting in activation of one or more oncogenes (Renan 1990). The promotion stage describes the conversion of an initiated cell from a premalignant phenotype to a malignant one, perhaps through the inactivation of a second type of gene called a tumor-suppressor gene, and, finally, progression is the stage of more aggressive tumor growth (Renan 1990). When radiation is acting as the carcinogen, the type of mutagens may vary widely. Photon irradiations are observed to involve point mutations (Renan 1990), and we should expect gross rearrangements and deletions in DNA to occur following HZE exposures. The GCR spectrum imposes further difficulties because of the broad range of ion velocities and charge number that occur and because of the protracted exposure encountered on a long space mission.

Several mathematical models of initiation and promotion have been developed for phenomenological descriptions of carcinogenesis, including models of natural incidence of cancer (Moolgavkar and Knudson 1981) and radiation carcinogenesis following exposures to radon (Moolgavkar et al. 1990) or alpha emitters (Marshall and Groer 1977). The works of Marshall and Groer (1977) and Moolgavkar et al. (1990) consider the effects of division and differentiation on initiated cells in order to provide a parametric description of the age-specific incidence. Models that undertake similar descriptions of cancer from GCR exposures must consider the continuum of carcinogens entailed in the broad distribution of charge and energy of these ions and the success of HZE particles for cell inactivation as observed in cell culture

studies. Dose-response curves for tumor induction are often parameterized as (Upton 1986)

$$I = (c_0 + c_1 D + c_2 D^2) e^{-(b_1 D + b_2 D^2)} \quad (1)$$

where  $I$  is the tumor occurrence,  $D$  is the absorbed dose,  $c_0$  is the natural occurrence of cancer,  $b_1$  and  $b_2$  are the linear and quadratic coefficients, respectively, for high-dose saturation, and  $c_1$  and  $c_2$  are the linear and quadratic coefficients, respectively. The exponential factor in equation (1) accounts for saturation or decrease in the occurrence at higher doses which is often attributed to cell inactivation. The usefulness of equation (1) for HZE exposures is severely limited if methods are not available for determining the dependence of the parameter on radiation quality. The track-structure model of Katz et al. (1971) has been successful in providing a parametric approach for considering HZE effects with accurate predictions made for an arbitrary ion species provided from fits to experimental data for  $\gamma$ -rays and a few ion types. Typically, the Katz model is considered only for acute exposures. More recently, a model of linear repair and misrepair kinetics has been developed by Wilson, Cucinotta, and Shinn (1993) which includes the Katz action cross-section formalism and provides a description of temporal effects and the competition on a cell population between inactivation and mutations. In this paper, we extend the kinetics model to include the assumption of initiation and promotion assumption in order to develop a parametric model of HZE carcinogenesis.

The first purpose of this paper is to provide a model-dependent formalism that is the age-dependent analogy of equation (1) which should be useful for parametric descriptions of GCR effects based on the success of the Katz action cross-section model. This presupposes that the description of Katz for cell damage as described in the terminology of grain count, track width, and thindown carries over to cancer in animals from cellular stud-

ies. A second purpose is to consider fractionated exposures, in particular, the role of cell inactivation and radiation induction of a second mutation of an initiation-promotion model.

High-linear-energy-transfer (LET) ions have shown an inverse dose-rate effect in which fractionated or protracted exposures are often more severe than acute exposures (Ullrich, Jernigan, and Storer 1977; Ullrich 1984). The experiments of Ullrich suggest that for animal systems, protracted exposures with high-LET radiations participate in the promotion stage of carcinogenesis. Exposure with fission neutrons shows that the inverse dose-rate effect is tissue dependent as well as dose dependent (Ullrich, Jernigan, and Storer 1977). In cell-culture studies, synchronization experiments suggest that a sensitive window in the cell cycle exists (Hill et al. 1982; Brenner and Hall 1990). However, we do not know if the same explanation will be true in animal systems in which the length of the cell cycle is typically much longer than that in culture. Finally, we consider model predictions for temporal effects for the relative biological effectiveness of high-energy Fe and protons in which the effects of nuclear reactions or target fragments are included. In particular, we consider any age dependence on the relative biological effectiveness.

In the remainder of this paper, we first review the kinetics model of multiple-radiation-induced lesions and repair and misrepair of the lesions, including the introduction of the track-structure model. We next introduce a basic model of growth kinetics for initiated cells and obtain expressions for tumor prevalence. Dose fractionation is then considered in our model, including the possibility of radiation induction of a mutation that we associate with the promotion stage of carcinogenesis. Finally, we discuss fits to the experiments for Harderian-gland-tumor prevalence and discuss model predictions for dose fractionation.

## Kinetics Model for Initiation

A kinetics model for cellular repair and misrepair has been developed by Wilson, Cucinotta, and Shinn (1993) that includes multiple-lesion formation and is based on first-order repair kinetics. First-order kinetics models have been considered previously by Dertinger and Jung (1970) and Dienes (1966) for survival curves following photon exposures. This development of Wilson et al. includes multiple-lesion types, such as those related to cell inactivation and mutation, and utilizes the track-structure model of Katz et al. (1971) for modeling the lesion-formation rates for charged particles. We note that other forms of enzyme kinetics, including zeroth order, second order, or mixed orders, can be considered. The use of first-order kinetics offers at least the simplicity of analytic solutions and provides a parametric framework.

The kinetics model assumes that nascent lesions are active chemical species produced in fast processes by radiation. The active chemical species, also denoted as substrates, are acted upon by enzymes in the cell and eventually repair to their original state or are misrepaired and left in a permanent damaged state. The fixation of the nascent lesions is assumed to occur over a time scale of minutes to hours and to follow first-order kinetics. As is well accepted in radiation biophysics, we have two distinct time scales, one for the initial events and another for the subsequential fixation of lesions. The uninjured population of cells at time  $t$  is denoted by  $n_0(t)$ . The number of cells at time  $t$  with locus  $l$  damaged with a number  $i$  of lesions is denoted by  $n_{li}(t)$ . The production of these lesions by radiation is described by rate constants  $k_{li}$ , which will be dependent on radiation type (for example, the charge and velocity of an ion). The ability of the cell to repair damage leads to a rate of repair of the  $n_{li}$  denoted  $\alpha_{rli}$ , and if the active species are stabilized but left in a misrepaired state, a misrepair rate  $\alpha_{mli}$  occurs. (The rates for lesion formation and repair and misrepair are in units of inverse time.) The balance equations for the time development of cell populations in a single phase of the cell cycle are then given for the uninjured population (Wilson, Cucinotta, and Shinn 1993) as

$$\dot{n}_0(t) = \sum_{li} \alpha_{rli} n_{li}(t) - k n_0(t) \quad (2)$$

for a locus left in a misrepaired state as

$$\dot{n}_l(t) = \sum_i \alpha_{mli} n_{li}(t) + \sum_{l'i'} \alpha_{rli'} n_{ll'i'}(t) - k n_l(t) \quad (3)$$

and for the number of cells with  $l$  and  $i$  as

$$\dot{n}_{li}(t) = \sum_{l'i'} \alpha_{rli'} n_{ll'i'}(t) + k_{li} n_0(t) + \sum_{j=1}^{i-1} k_{li-j} n_{lj}(t) - k n_{li}(t) - \alpha_{li} n_{li}(t) \quad (4)$$

In equation (4),  $n_{ll'i'}(t)$  denotes the cells with lesions at two loci which obey similar rate equations, and we define

$$\alpha_{li} = \alpha_{rli} + \alpha_{mli} \quad (5)$$

and

$$k = \sum_{li} k_{li} \quad (6)$$

We consider only the mutation or mutations at the loci associated with initiation with those cells left permanently fixed in this state denoted by  $n_I(t)$ . In order to proceed, loci associated with clonogenic death must be considered because the mutation phenotype must be expressed in a hereditary fashion. The radiation induction rates associated with clonogenic death are denoted by  $k_{di}$  with

$$k_d = \sum_i k_{di} \quad (7)$$

The radiation induction rates associated with the initiation mutation are denoted by  $k_{Ii}$  with

$$k_I = \sum_i k_{Ii} \quad (8)$$

The solution of rate equations (2)–(8) for acute exposures follows if we exploit the time scales for the fast radiation processes and subsequent fixation. Convergence in the dose range below 10 Gy is achieved for  $i \leq 3$ , and we assume a value of 3 for both clonogenic death and mutations. The solution for survival after repair is complete (Wilson, Cucinotta, and Shinn 1993) and is given by

$$n_0(t) = n_0(0) e^{-k_d t r} + \sum_{i'=1}^{m_d-1} \frac{\alpha_{rdi'}}{\alpha_{di'}} \left[ n_{di'}(t_r) + \sum_{i=1}^{\infty} \left( \frac{\alpha_{rli} + \alpha_{rdi'}}{\alpha_{li} + \alpha_{di'}} \right) n_{Iidi'}(t_r) \right] \quad (9)$$

and for initiation by

$$n_I(t) = \left( e^{k_I t_r} - 1 \right) \left[ e^{-k t_r} n_0(0) + \sum_{i'=1}^{m_d-1} \frac{\alpha_{rdi'}}{\alpha_{di'}} n_{di'}(t_r) \right] - \sum_{i'=1}^{m_d-1} \frac{\alpha_{rli}}{\alpha_{li'}} \left[ n_{Ii}(t_r) + \sum_{i'=1}^{m_d-1} \frac{\alpha_{rdi'}}{\alpha_{di'}} n_{Iid'}(t_r) \right] \quad (10)$$

where  $m_d = 3$ ,  $m_I = 3$ ,  $t_r$  is the duration time of the exposure, and where

$$\left. \begin{aligned} n_0(t_r) &= n_0(0) e^{-k t_r} \\ n_{d1}(t_r) &= k_{d1} t_r n_0(0) e^{-k t_r} \\ n_{d2}(t_r) &= \left( k_{d2} t_r + \frac{1}{2!} k_{d1}^2 t_r^2 \right) n_0(0) e^{-k t_r} \\ n_{d3}(t_r) &= \left( k_{d3} t_r + \frac{2}{2!} k_{d2} k_{d1} t_r^2 + \frac{1}{3!} k_{d1}^3 t_r^3 \right) n_0(0) e^{-k t_r} \\ n_{I1}(t_r) &= k_{I1} t_r n_0(0) e^{-k t_r} \\ n_{I2}(t_r) &= \left( k_{I2} t_r + \frac{1}{2!} k_{I1}^2 t_r^2 \right) n_0(0) e^{-k t_r} \\ n_{I1d1}(t_r) &= \frac{2}{2!} k_{I1} k_{d1} t_r^2 n_0(0) e^{-k t_r} \\ n_{I1d2}(t_r) &= \left( \frac{2}{2!} k_{I1} k_{d2} t_r^2 + \frac{3}{3!} k_{d1}^2 k_{I1} t_r^3 \right) n_0(0) e^{-k t_r} \\ n_{I2d1}(t_r) &= \left( \frac{2}{2!} k_{d1} k_{I2} t_r^2 + \frac{3}{3!} k_{I1}^2 k_{d1} t_r^3 \right) n_0(0) e^{-k t_r} \end{aligned} \right\} \quad (11)$$

The possibility of radiation acting as both initiator and promoter suggests the treatment of two specific mutation types. In the experiments studying tumor formation in the Harderian gland of a mouse (Fry et al. 1985; Alpen et al. 1993 and 1994), animals are exposed at about 100 days and we should expect few cells already initiated for radiation to act upon. For fractionated exposures, the number of initiated cells will increase through radiation as well as division, and we will include a second mutation related to promotion which we describe below. We next discuss the treatment of track structure following Katz et al. (1971) in the kinetics model.

### Track-Structure Model for Lesion Formation

The lesion-production coefficients in the kinetics model must include track-structure effects in order to describe HZE exposures. The model of Katz has been successful for many years in providing a parametric description of track structure and is used here to model the lesion-production rates. In the Katz model, biological damage from fast ions is assumed to be caused by secondary electrons ( $\delta$ -rays) produced along the path of the ion. The effects caused by energetic ions are correlated with those of  $\gamma$ -rays by assuming that the response in sensitive sites near the path of the ion is part of a larger system irradiated with  $\gamma$ -rays at the same dose level. The action cross section is the probability of single-particle (inactivation) activation or mutation and is calculated by integrating the  $\gamma$ -ray probability function over the radial path of the ion as

$$\sigma = 2\pi \int_0^{T_M} b db P(b) \quad (12)$$

where  $b$  is the radial distance from the ion to a sensitive site of characteristic size  $a_0$ ,  $T_M$  is the maximum  $\delta$ -ray range, and  $P(b)$  is a probability function for  $\gamma$ -ray response assumed to be of the multitarget or multihit form.

For example, in the multitarget model,

$$P(b) = \left[1 - e^{-\overline{D}(b)/D_0}\right]^m \quad (13)$$

where  $m$  is the target number,  $D_0$  is the  $\gamma$ -ray radiosensitivity parameter, and  $\overline{D}(b)$  is the average dose at the sensitive site. The cross section calculated in equation (12) is observed to plateau at a value  $\sigma_0$ , which is indicative of an effective damage area inside the nucleus. The cross section is observed to rise above the plateau value for stopping ions, which is referred to by Katz et al. (1971) as the track-width regime, and then to fall to zero, which is referred to as thindown. (See Katz, Dunn, and Sinclair 1985). For relativistic ions of moderate charge,  $\sigma < \sigma_0$ , and this is called the grain-count regime. In the track-structure model, a fraction  $1 - (\sigma/\sigma_0)$  of the fluence of the ion is assumed to be available to act through intertrack effects in a manner similar to  $\gamma$ -rays, and the gamma-kill dose of the ion is defined as

$$D_\gamma = \left(1 - \frac{\sigma}{\sigma_0}\right)D \quad (14)$$

with  $D_\gamma = 0$  if  $\sigma > \sigma_0$ , and  $D$  is the absorbed dose. In the grain-count regime, the action cross section is conveniently parameterized as

$$\sigma = \sigma_0 \left(1 - e^{-Z^*/\kappa\beta^2}\right)^m \quad (15)$$

where  $Z^*$  denotes the effective charge of the ion,  $\beta$  denotes the velocity, and  $\kappa$  is related to the parameters  $D_0$  and  $a_0$  through

$$\kappa = \frac{D_0 a_0^2 \times 10^{11}}{C} \quad (16)$$

where  $D_0$  is given in Gy,  $a_0$  is given in cm, and  $C$  is a constant that defines the average dose deposited in an extended target by an ion passing through that target. In the earlier work following the radial-dose model of Butts and Katz (1967), the constant  $C$  was set at 2. More recently, Chunxiang, Dunn, and Katz (1985) have considered a more accurate range-energy relationship for the maximum range of  $\delta$ -rays. Using this model of radial dose, we find that  $C \approx 0.7$ , which effectively reduces the radius  $a_0$  of the target by about 60 percent from earlier results using the Katz model.

The lesion-induction coefficients of the kinetics model are matched to the Katz model by Wilson, Cucinotta, and Shinn (1993) through the choices

$$k_{I3}t_r = \sigma_I F \quad (17)$$

$$k_{d3}t_r = \sigma_d F \quad (18)$$

where  $F$  is the fluence of the ion,  $\sigma_I$  and  $\sigma_d$  are the action cross sections for cell initiation and inactivation, respectively, and

$$\left. \begin{aligned} k_{I1}t_r &= 6^{1/3} \frac{D_{\gamma I}}{D_{0I}} \\ k_{d1}t_r &= 6^{1/3} \frac{D_{\gamma d}}{D_{0d}} \end{aligned} \right\} \quad (19)$$

with all other values of  $k$  set to zero. The choices in equations (17)–(19) assume that  $\gamma$ -rays achieve only a single step,  $k_{I1}$  or  $k_{d1}$ , whereas ions are capable of transition to the unreparable states with a probability of  $k_{I3}$  or  $k_{d3}$ . For low-LET ions at high energies, the effects of target fragments must be included, and this is achieved by summing over the energy spectrum of all secondary ions as described by Cucinotta et al. (1991).

## Summary of Parameters for Initiation Kinetics

In order to clarify the number and meaning of parameters introduced in the kinetics model, we briefly summarize these. For describing the dose-response curves for  $\gamma$ -rays, a radiosensitivity parameter denoted

by  $D_0$  is used with a distinct parameter for initiation ( $D_{0I}$ ) and survival ( $D_{0d}$ ). Repair rates and efficiencies also occur in the kinetics equations. For acute exposures and for fractionated exposures with interfractionation times much longer than the time scale of repair ( $>1$  day), only the repair efficiencies occur in the dose-response equations. In the model the cells that have sustained three or more nascent lesions are left fixed (repair efficiency is zero) as initiated cells or inactivated cells. This leaves two repair efficiencies as parameters with values between zero and unity which are denoted by  $\alpha_{rd1}/\alpha_{d1}$  and  $\alpha_{rd2}/\alpha_{d2}$  for cell survival and by  $\alpha_{rI1}/\alpha_{I1}$  and  $\alpha_{rI2}/\alpha_{I2}$  for initiation. The misrepair efficiencies are then determined as unity minus the repair efficiency. The repair efficiency for cells with one lesion is most important for fitting the dose-response curve, and this together with  $D_0$  determine the initial slope of the  $\gamma$ -rays (Wilson, Cucinotta, and Shinn 1993), which is zero for 100-percent repair efficiency.

For describing the response to track-segment irradiations with charged ions, we also require action cross sections for both the cell inactivation and the initiation mutation. These are modeled by using the parametric track-structure model of Katz. Here, the response for any charged ion is determined from a knowledge of the radiosensitivity parameter for  $\gamma$ -rays for the identical end point, the average radial dose in a sensitive volume of radius  $a_0$ , and an effective target area  $\sigma_0$  that encloses the sensitive volumes. By using equation (12), the action cross sections are then determined by fitting the values  $a_0$  and  $\sigma_0$  to a data set as described by Katz et al. (1971). The cross sections for survival and initiation are distinct and result in two new parameters  $a_{0d}$ ,  $a_{0I}$  and  $\sigma_{0d}$ ,  $\sigma_{0I}$  for each end point which are fit to dose-response curves. In practice, equation (15) is used for particles in the grain-count regime, with the result that the parameter  $\kappa$  is used as the fitting parameter and  $a_0$  is then determined by equation (16). For mixed-radiation fields (i.e., to include the effects of target fragments produced by high-energy ions), the contributions from all nuclear secondaries are summed to define an effective cross section as described by Cucinotta et al. (1991).

## Growth Kinetics and Tumor Prevalence

In the two-mutation model of initiation promotion, the number of initiated cells must be specified as a function of tissue age. Here, the effects of division and differentiation of initiated cells are important for describing age-response curves (Moolgavkar and Knudson 1981). For describing the natural incidence, the kinetics equation for the normal cell population is assumed to be

$$\dot{n}_0(t) = (-\mu_I - \beta_0 + \gamma_0)n_0(t) \quad (20)$$

where  $\mu_I$  is the natural rate of initiation,  $\beta_0$  is the rate of cell loss, and  $\gamma_0$  is the rate of cell division with all rates in units of  $\text{day}^{-1}$ . The initiated cell population ( $n_I(t)$ ) is determined by

$$\dot{n}(t) = \mu_I n_0(t) - (\mu_P + \beta_I - \gamma_I)n_I(t) \quad (21)$$

where  $\mu_P$  is the natural rate of promotion,  $\beta_i$  is the rate of cell loss for  $n_I$ , and  $\gamma_I$  is the rate of division of initiated cells. The time rate of change of promoted cells is given by

$$\dot{n}_P(t) = \mu_P n_I(t) \quad (22)$$

The rates for initiation, promotion, division, and cell loss in equations (20)–(22) may have some time dependence; however, they are assumed to be constant here. For the normal cell population, we will assume that most of the cells are quiescent (i.e., in the  $G_0$  phase) and that losses are small, such that

$$n_0(t) = s e^{-\mu_I t} \approx s \quad (23)$$

where the initial population is denoted by  $n_0(0) = s$ . The solution for the initiated population with the initial condition  $n_I(0) = 0$  is then

$$n_I(t) = \frac{\mu_I s}{\gamma_I - \beta_I + \mu_I - \mu_P} [\exp(\gamma_I - \beta_I - \mu_P)t - \exp(-\mu_I t)] \quad (24)$$

For  $\gamma_I - \beta_I \gg \mu_I$  or  $\mu_P$ , the rate of growth is controlled by  $\gamma_I - \beta_I$ .

The tumor prevalence is scored as the number of animals in which a neoplasm is found divided by the number of animals at risk at time  $t$ . In the kinetics model, the number of promoted cells is determined by equation (22) from which we define the hazard function (Marshall and Groer 1977) or rate of appearance of tumors as

$$h(t) = \dot{n}_P(t - g) \quad (25)$$

where  $g$  is the minimum tumor growth time, which is some minimal time necessary for observing a tumor. The prevalence is then given by

$$P(t) = 1 - \exp\left(-\int_0^t h(t) dt\right) \quad (26)$$

We next include the effects of radiation induction of initiated cells for the case of acute exposures. The time scale of induction of lesions by radiation is certainly less than a fraction of a second. Enzymatic repair and misrepair of the lesions are observed to be complete in a few days, although for cancer induction, the state of knowledge is not well known. The kinetics of tissue growth will occur over a much longer time, perhaps many days, and we assume that the differences in time scales of these kinetic processes are such that they may be treated independently in a sequential manner. The effects of radiation and repair on  $n_0(t)$  and  $n_I(t)$  are given by equations (8) and (9), respectively. By letting  $t_r$  be the time of exposure,  $n_0(t_r)$  and  $n_I(t_r)$  be the number of normal and initiated cells immediately after exposure and repair are complete, respectively, and having irradiation occur early in the animal's lifetime, we find that

$$\begin{aligned} \dot{n}_P(t) = & \frac{\mu_I \mu_P n_0(t_r)}{\gamma_I - \beta_I + \mu_I - \mu_P} \{\exp[\gamma_I - \beta_I - \mu_P](t - t_r)\} \\ & \times \exp(-\mu_I t_r) - \exp(-\mu_I t) + \mu_P n_I(t_r) \exp[\gamma_I - \beta_I - \mu_P](t - t_r) \end{aligned} \quad (27)$$

The second term in equation (27) thus represents radiation-induced, initiated cells. An important question for modeling is whether radiation significantly modifies the growth of initiated cells. Here, we use the growth constant  $\gamma_I - \beta_I$  from natural-incidence curves as a first estimate. Radiation will initially cause a blocking of progression through the cell cycle; however, the delay time should be small compared with the length of time elapsed before the observation of cancer, which is usually several hundred days. We note that experimental studies with  $\gamma$ -rays and neutrons show similar slopes for age versus incidence with the time of appearance shortened for high-LET radiations (NCRP 1990). We also note that the solutions given above for tumor prevalence versus time rely only on the combination  $\gamma_I - \beta_I$ , and not on these parameters individually.

## Results for Fluence-Response Curves

Tumor prevalence in the Harderian gland of B6CF<sub>1</sub> female mice after radiation exposure has been measured (Fry et al. 1985; Alpen et al. 1993) using pituitary hormones to increase the rate of expression. The exposures included  $\gamma$ -rays and several relativistic ions. Animals were exposed at an age near 100 days and were sacrificed at 600 days. The initial number of cells is about  $5 \times 10^6$  per gland with a nuclear diameter of about  $5.5 \mu\text{m}$  (according to a private communication with Fry in 1992), and we have assumed that about two-thirds of the cells are susceptible, with the result that the initial cell population is estimated at  $s = 2/3 \times 5 \times 10^6$ . In figure 1 (see the dotted-line curve) we have fit the model of equation (26) to the data for natural incidence with pituitary isografts. The data are from Fry et al. (1985) and from a private communication with Fry in 1992, and the curves represent the choice for the parameters that are listed in table 1. The minimum growth time was set at 100 days with results not very sensitive to choices up to about 200 days. The limited amount of data was not sufficient to rigorously define the parameters; however, they are constrained to within about a factor of 2 for the model under study.

Table 1. Model Parameters for Harderian Gland Tumors

(a) Natural-incidence parameters

$\mu_I$ , per day . . . . .	$1 \times 10^{-7}$
$\mu_P$ , per day . . . . .	$1 \times 10^{-7}$
$\gamma_I - \beta_I$ , per day . . . . .	$6 \times 10^{-3}$

(b) Radiation-induction parameters

End points	$\sigma_0$ , $\text{cm}^2$	$\kappa$	$m$	$D_0$ , Gy
Survival . . . . .	$3.2 \times 10^{-7}$	550	3	3.2
Initiation . . . . .	$7.6 \times 10^{-10}$	480	3	148.0

(c) Repair efficiencies

End points	Values of $\alpha_{ri}/\alpha_i$ for—	
	$i = 1$	$i = 2$
Inactivation . . . . .	0.999	0.5
Initiation . . . . .	0.995	0.5

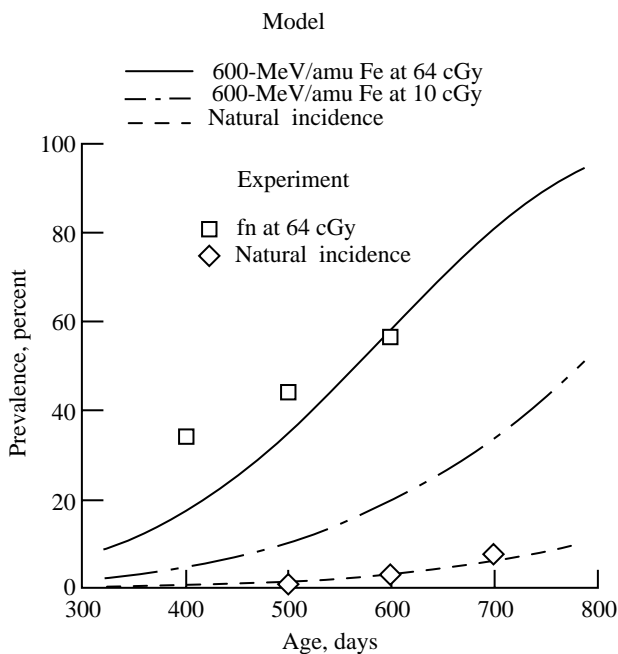


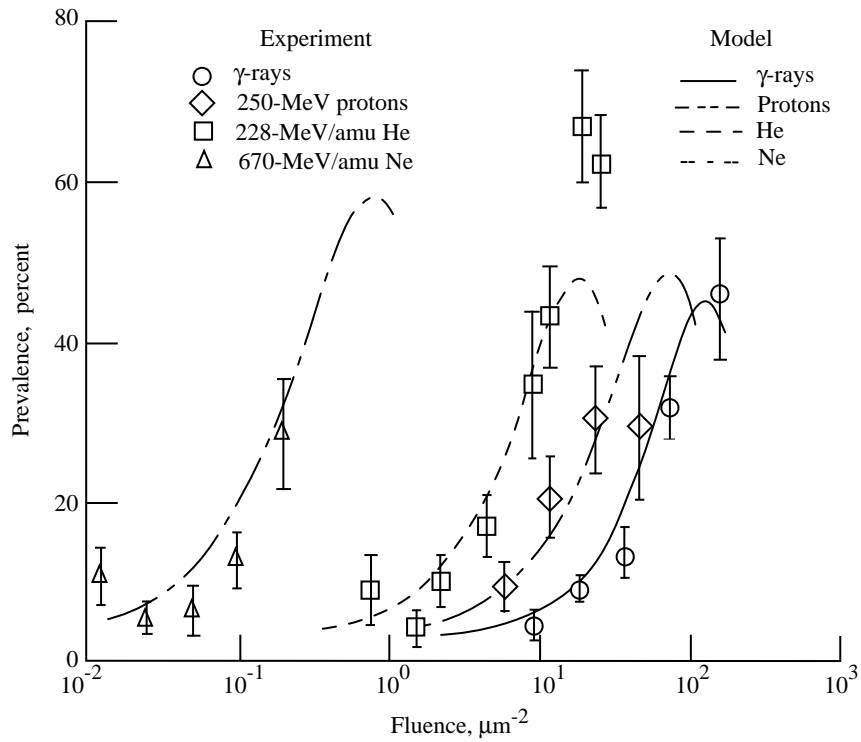
Figure 1. Prevalence plotted against age of mice at risk for Harderian gland tumors using pituitary isografts.

In figure 2, fits to the data of Alpen et al. (1993) for tumor prevalence using equations (25)–(27) and (10) are shown versus particle fluence. An LET value of  $0.23 \text{ keV}/\mu\text{m}$  is assumed for  $\gamma$ -rays. A summary of the ion types and their energies and lin-

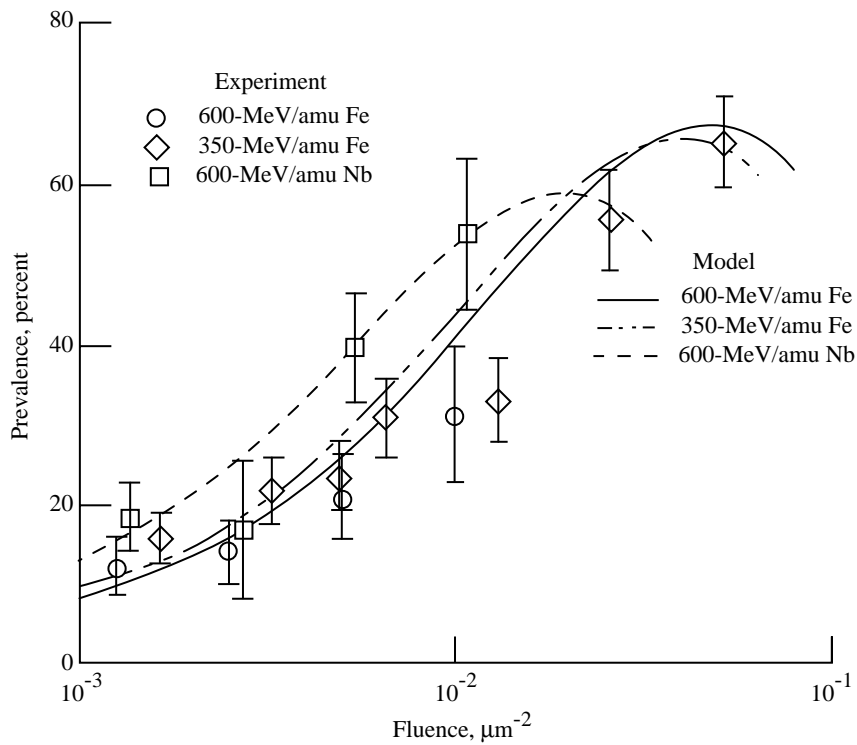
ear energy transfers are given in table 2. Calculated values are also given in table 2 using equations (12) or (15) for the action cross sections for cell inactivation and initiation with the fitted parameters for radiosensitivity and action cross sections in table 1. The repair efficiencies are also listed in table 1. The error bars in figure 2 denote the standard deviations of the prevalence reported by Alpen et al. (1993). Overall, the agreement with the data is good for all but two data points fitted to within the experimental 95-percent confidence intervals (Alpen et al. 1993).

For the  $^1\text{H}$  and  $^4\text{He}$  exposures, the effects of target fragmentation were included following the method described by Cucinotta et al. (1991), and their contributions to  $\sigma$  are listed in parentheses in table 2. The target fragments represent a substantial increase in the prevalence as compared with the  $\gamma$ -ray response for these low-LET ions, as can be seen in figure 2(a). The  $^4\text{He}$  response, however, is underpredicted at the higher fluences. The present model offers no explanation for the differences seen between  $^1\text{H}$  and  $^4\text{He}$  at large fluences. The model predicts and the data suggest a turn-down in the prevalence at large fluence for  $^4\text{He}$  which we attributed solely to cell killing, thus reducing the number of target cells available for initiation.

For the Nb exposure, the cross section is calculated through integration over the radial distance using equation (12) because the fit equation is not



(a) Low-to-medium LET radiations.



(b) High-LET radiation.

Figure 2. Prevalence of Harderian gland tumors at age of 600 days plotted against particle fluence. Experimental data are taken from Alpen et al. (1993). Error bands represent standard deviations.

Table 2. Radiation Types and Action Cross Sections of Tumor Prevalence in Harderian Gland

Radiation type	Energy, MeV/amu	LET, keV/ $\mu\text{m}$	$\sigma_I$ , $\text{cm}^2$ (a)	$\sigma_d$ , $\text{cm}^2$ (a)
$^1\text{H}$	250	0.4	$1.3 \times 10^{-16}$ ( $5.0 \times 10^{-14}$ )	$3.6 \times 10^{-14}$ ( $1.9 \times 10^{-11}$ )
$^4\text{He}$	228	1.6	$9.7 \times 10^{-15}$ ( $1.0 \times 10^{-13}$ )	$2.7 \times 10^{-12}$ ( $3.8 \times 10^{-11}$ )
$^{20}\text{Ne}$	670	25	$1.5 \times 10^{-11}$	$4.5 \times 10^{-9}$
$^{56}\text{Fe}$	600	193	$5.4 \times 10^{-10}$	$2.0 \times 10^{-7}$
$^{56}\text{Fe}$	350	253	$6.5 \times 10^{-10}$	$2.5 \times 10^{-7}$
$^{93}\text{Nb}$	600	464	$1.0 \times 10^{-9}$	$5.0 \times 10^{-7}$

<sup>a</sup>Values in parentheses represent target-fragment contributions.

Table 3. Cellular-Response Parameters for Survival in Mammalian Cell Lines

Cell type	$\sigma_0$ , $\text{cm}^2$	$\kappa$	$m$	$D_0$ , Gy
Harderian gland . . . . .	$3.2 \times 10^{-7}$	550	3	3.2
C3H10T1/2 . . . . .	$5.0 \times 10^{-7}$	750	3	2.8
V-79 . . . . .	$4.28 \times 10^{-7}$	1100	3	1.82
T-1 kidney cells . . . . .	$6.7 \times 10^{-7}$	750	2.5	1.7
HeLa . . . . .	$5.6 \times 10^{-7}$	1100	3	3.7
Mouse bone marrow . . . . .	$4.2 \times 10^{-7}$	500	2.5	0.9

accurate in the track-width regime. We note that no reduction in carcinogenic potential is expected from the highest LET ions for the ions under study in the present model because of their relatively high velocities. For stopping ions which have similar LET as the Nb beam, the model would predict such a reduction. The parameters obtained for the initiation cross section (table 2) estimate an effective area  $\sigma_0$  slightly larger than that seen in mutation studies (Tsuboi, Yang, and Chen 1992) or transformation studies *in vitro* (Yang et al. 1985) which suggests that several genes are able to act as initiators.

Transplantation studies of Harderian gland cells from CBA/Cne mice into the fat pads of isogenic recipients were studied by Di Majo et al. (1986) where *in vivo* survival curves were measured following X-ray irradiation. The age of the mice at exposure was approximately the same as the ages used by Fry et al. (1985) and Alpen et al. (1993). Although the mice are of a different strain and the experiments of Alpen et al. (1993) used a  $\gamma$ -ray source for the reference radiation, we compare their survival measurements in figure 3 with the model survival curves that result from our model as given by equation (9). The agreement is good, but the relevance is uncertain for the reasons stated. Although *in vivo* measurements (us-

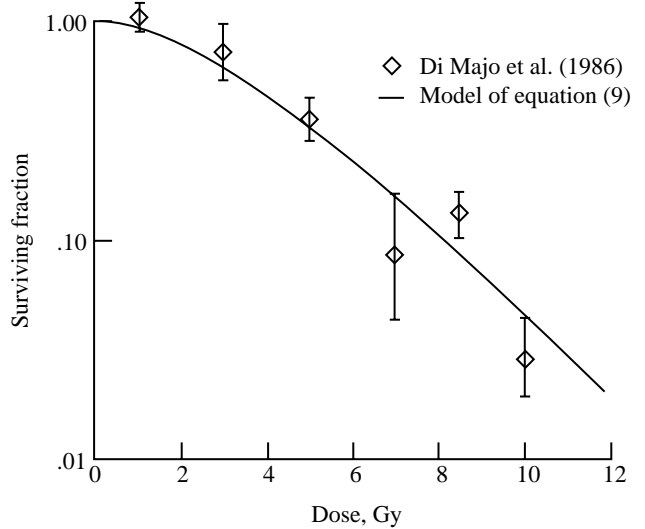


Figure 3. Survival plotted against absorbed dose in Harderian gland tissue. Experimental data are taken from Di Majo et al. (1986) for CBA/Cne mice using X-ray irradiations. Error bands represent standard deviations.

ing charged particles) for this tissue are not available, we note that the cellular-response parameters for survival listed in table 1 are similar to those fitted by the

Katz model for many mammalian cell lines, which, for comparison, are listed in table 3. Cell killing has an important effect on the tumor prevalence measured at intermediate and large doses for heavy ions and cannot be ignored in model predictions of tumor induction.

### Age Effects and Role of Pituitary Isografts

In figure 1, we have calculated the tumor prevalence as a function of age for the 600-MeV Fe exposure at doses of 10 and 64 cGy. Also plotted are data for a fission neutron (fn) exposure with a mean neutron energy of 0.85 MeV at a dose of 64 cGy. Calculations were not performed for the fn exposure at this time because of the detailed transport analyses required. The similarity in the time development for Fe and fn is quite noticeable, with the slope of the model calculations for the prevalence curve for Fe being more rapid than that of the experiments with fission neutrons. We noted that an identical slope could be achieved by using a decrease in the growth rate with a corresponding increase in the spontaneous promotion rate. The comparison in figure 1 suggests that using the value  $\gamma_I - \beta_I = 6 \times 10^{-3}$  per day fitted to the natural-prevalence curve for radiation-induced tumors is fairly accurate for the system under study. The use of pituitary hormones is expected to increase the growth parameter  $\gamma_I - \beta_I$  over the natural rate in the two-mutation model. Exposures were also performed for Fe (Alpen et al. 1993) and fn (Fry 1981) without the use of pituitary isografts. In both cases, a decrease appeared in occurrence; however, for the Fe exposures, the decrease was small. We fit our model to the data of Grahn, Lombard, and Cranes (1992) for the natural prevalence of Harderian gland tumors without isografts and found a value of  $\gamma_I - \beta_I \approx 2.7 \times 10^{-3}$  per day if we keep  $\mu_I$  and  $\mu_P$  fixed as in table 1. The data for Fe without isografts can be fit in our model with  $\gamma_I - \beta_I = 3.5 \times 10^{-3}$  per day if all other parameters are unchanged.

In figure 4, we show calculations of the relative biological effectiveness (RBE) for  $^1\text{H}$  at 250 MeV and  $^{56}\text{Fe}$  at 600 MeV/amu as a function of age for an excess prevalence of 3 percent. The calculations suggest that for acute exposures, the RBE is sensitive to age with an RBE increase with age due to the reduced role of cell inactivation in achieving a 3-percent excess prevalence at the later ages for these ions.

### Dose Fractionation and Promotion By Radiation

Many experimental studies in animals as well as in cell culture observe an enhancement in oncogenic re-

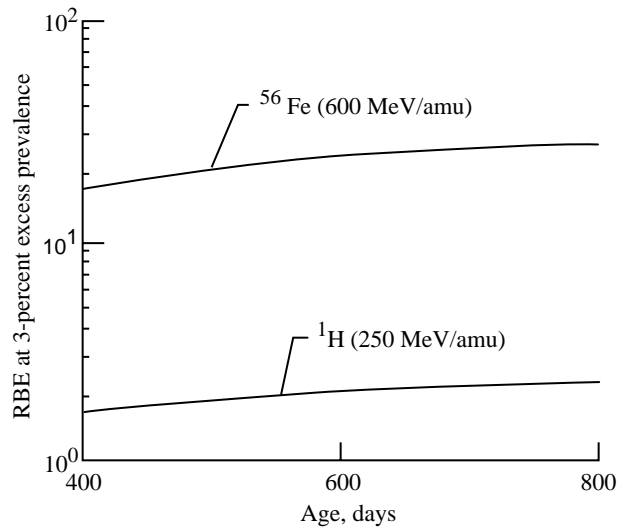


Figure 4. RBE at 3-percent excess prevalence for Harderian gland tumors plotted against age of mice exposed at 100 days. Model calculations are for  $^{56}\text{Fe}$  and  $^1\text{H}$ .

sponse for protracted or fractionated exposures with high-LET radiations. This is in contrast to photons where a sparing effect is observed as the norm. Several of the possible explanations for the enhancement or inverse dose-rate effect include a sensitive phase in cell cycle, the effects of reduced cell killing for protracted exposures as compared with acute exposures, the role of repopulation for tissue systems, and, finally, the possibility that radiation will act as a promoter of initiated cells. The recent experiments of Miller et al. (1990) using synchronized C3H10T1/2 cells establish that a sensitive phase exists for the transformation of cell cultures. For *in vivo* carcinogenesis, a large amount of data (Upton 1986; Ullrich, Jernigan, and Storer 1977; Ullrich 1984) performed under varying exposure conditions suggest that several factors contribute to the inverse dose-rate effect.

In principle, the kinetic equations in equations (2)–(11) could be extended to include the cell cycle (Wilson, Cucinotta, and Shinn 1993), as well as a second mutation type corresponding to promotion which could be interpreted as the activation of a tumor-suppressor gene. Such an approach would be cumbersome because of the need for a numerical solution of the resulting differential equations and because of the large number of parameters that would be required. Instead, we will consider fractionated exposures with interfractionation times longer than a few days in which analytic solutions are possible without the addition of many new parameters. This

allows us to consider several of the proposed explanations of the inverse dose-rate effect in the present model.

The roles of cell killing and repopulation are considered for a fractionated exposure separated by time intervals of a few days or more by sequential solution to equations (2)–(4) and (20)–(22). Here, the number of initiated cells from radiation at time  $t$  after  $N$  fractions for the case of no radiation-induced promotion is

$$n_I(t) = \sum_{i=1}^N n_I(t_i) \exp[(\gamma_I - \beta_I - \mu_P)(t - t_i)] f_i \quad (28)$$

where  $n_I(t_i)$  is the number of cells initiated by radiation in the  $i$ th fraction and  $f_i$  is the fraction of cells remaining after the  $i$ th fraction. To consider an upper bound on fractionation effects from possible repopulation between exposures, we also consider setting  $f_i$  equal to unity which corresponds to the case of full repopulation.

We will also consider a second mutation event corresponding to the promotion of initiated cells in fractionated exposures. This type of assumption becomes important for older ages in which the number of cells initiated spontaneously will be relatively large. Here, the kinetic equation solution follows from equations (2)–(4) with the introduction of a second mutation type that is active only in the initiated cells. If we assume that the populations  $n_I$  and  $n_P$  are always small compared with  $n_0$ , we find that the number of radiation-induced promoted cells in an  $N$ -fraction experiment is given by

$$n_P(t) \approx \sum_{i=2}^N n_I(t) \frac{n_P(t_i)}{n_I(t)} \quad (29)$$

where  $n_P(t_i)/n_I(t)$  represents the fraction of initiated cells promoted by the  $i$ th exposure and is given by equation (10), with the lesion formation rates and repair rates for promotion used instead of those for initiation. We estimate these rates in the following comparisons.

Figure 5 shows four calculations for fractionated exposures separated by 1 week of 600-MeV/amu Fe and  $\gamma$ -rays versus absorbed dose. In figure 5(a), we use equation (28) with no allowance for repopulation

between fractions. Two effects are observed: (1) the  $\gamma$ -rays show considerable sparring with increasing number of fractions, and (2) for Fe, a 24-week fractionated exposure also shows considerable sparring that is due to the initiated cells in the later fractions having insufficient time to divide before the sacrifice at 600 days. In figure 5(b), we allow for full repopulation between exposures. Again, the  $\gamma$ -rays show sparring. For Fe, an inverse dose-rate effect occurs for the two- and six-fraction schedules; however, for the 24-week schedule, the increase is seen only above 0.8 Gy with sparring again at the lower dose levels. The inverse dose-rate effect seen in fission neutron exposures for many tumor types shows a continued increase for even 60-week schedules (Grahn, Lombard, and Cranes 1992). Because we also do not expect full repopulation to occur, we expect that figure 5(b) does not account for the enhancement anticipated.

In figure 5(c), we include a second mutation rate from equation (29) and have all lesion formation parameters set equal to those used for initiation. A large enhancement is now seen for the fractionated exposures with a decrease for  $\gamma$ -rays again. With the fractionation combined with the mutation rate, we have assumed that the second mutation accounts for an inverse dose-rate effect. As a final estimate, we have considered calculations in figure 5(d) in which the promotion lesion is assumed to be similar to the HGPRF (hypoxanthine guanine phosphoribosyl transferase) mutation as estimated in our mutation model from the data of Tsuboi, Yang, and Chin (1992) and Thacker, Stretch, and Stephens (1979). Here  $\sigma_{0P} = 0.9 \times 10^{-10} \text{ cm}^2$  and  $D_{0P} \approx 1000 \text{ Gy}$ . For this very specific gene mutation, the enhancement is seen, although it is less significant than it would be if the promotion mutation rate were near that of initiation.

In space, the dominant radiation component is high-energy protons in which a flux of about  $2 \times 10^8$  protons/cm<sup>2</sup>/year is expected. Because these protons will produce an appreciable number of high-LET secondaries, we consider if an inverse dose-rate effect will occur for protracted exposure. In figure 6, we show calculations for 250-MeV protons using the model of figure 5(c). A large enhancement is seen above doses of 0.5 Gy, which is close to the expected dose on an extended space mission.

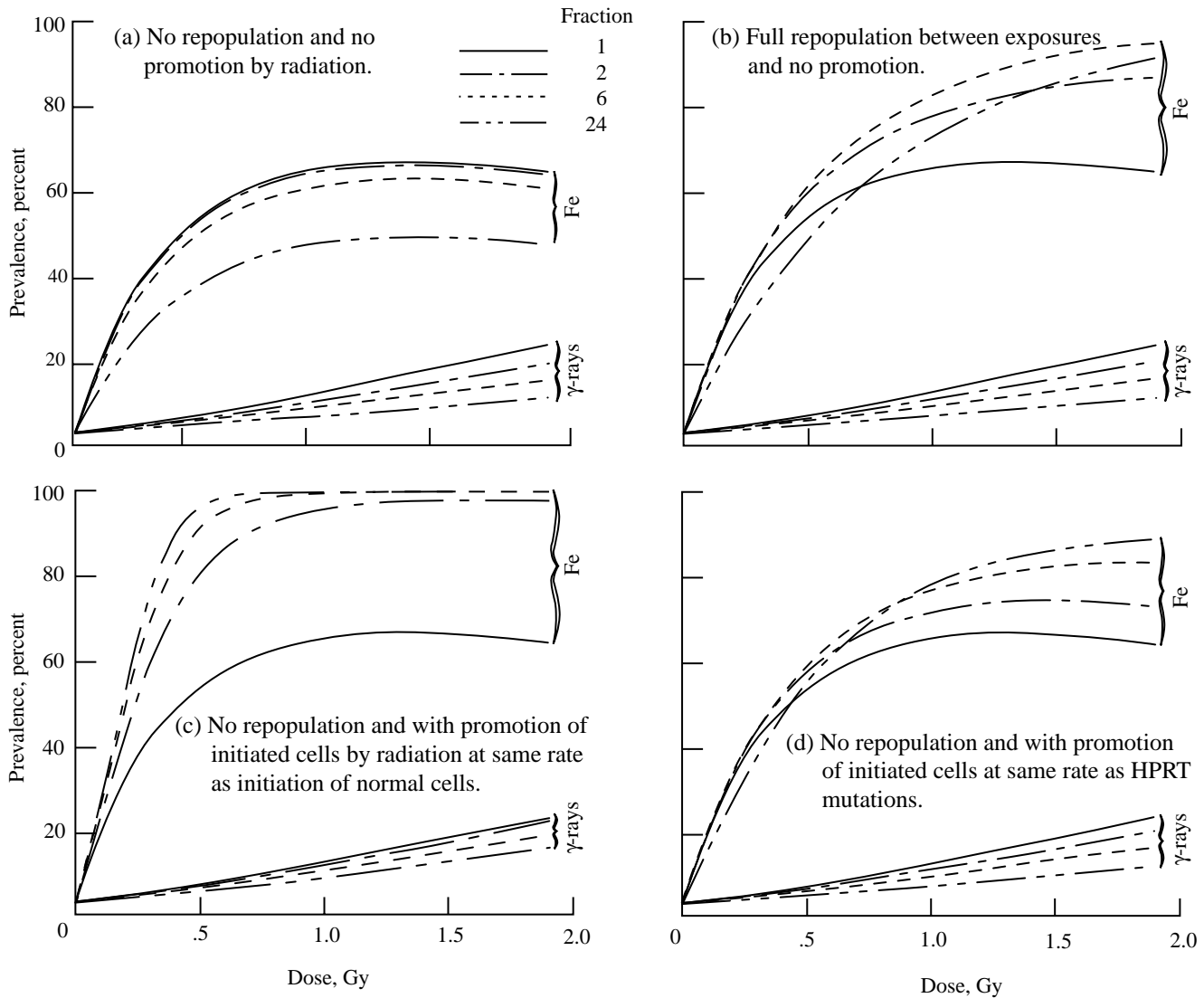


Figure 5. Model calculations of dose fractionation for Fe at 600 MeV/amu and  $\gamma$ -rays. Interfractionation times are 1 week.

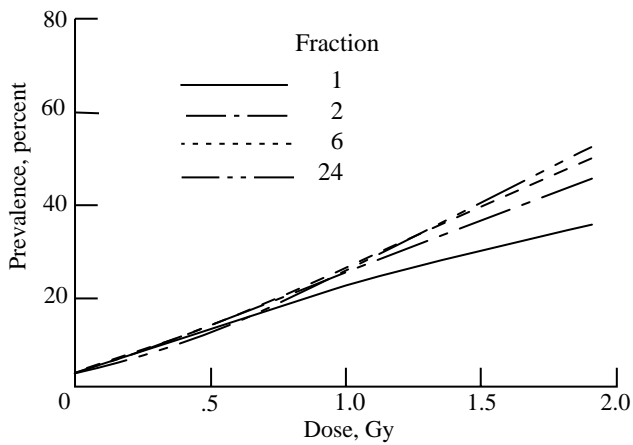


Figure 6. Model calculations of dose fractionation similar to figure 5(c) for 250-MeV protons.

## Concluding Remarks

By using the hypothesis that carcinogenesis in mice occurs through two mutational steps, we have developed a parametric model of radiation carcinogenesis for charged particles. The number or type of mutations required for cancer induction is not well known and is certainly not unique. By assuming a two-mutation model with clonal expansion of initiated cells, the age dependence of natural occurring tumors can be fitted, and the possibility of radiation-induced promotion can be explored. The model proceeds from the kinetics of lesion formation and repair and misrepair for the mutation and survival of cells. The use of linear-repair kinetics provides an analytic framework to consider dose-rate effects. However, many important questions regarding the kinetics of

enzymatic repair have not been considered, and these may become important in extrapolating a parametric model to low fluences. Track-structure effects have been introduced into our model through the use of the radial-dose formalism of action cross sections developed by Katz. The resulting parameterizations of action cross sections for mutations and inactivation as a function of charge and velocity of an ion allows for predictions for any monoenergetic or mixed field of radiation for which the particle-fluence spectrum is known.

A two-mutation model of the natural incidence of carcinogenesis requires rates for spontaneous production of the first and second mutations, as well as the rate of clonal expansion of the initiated cells that carry the first mutation. We have estimated these rates by using the natural-incidence curves for Harderian gland tumors in mice that have received pituitary isografts. The kinetics of radiation-induced mutation were coupled to the model of the natural incidence of cancer. For mice having acute exposures early in their mature life, we have assumed that the rate of expansion of initiated cells is close to the spontaneous rate. This assumes that the rate does not change appreciably with radiation type or damage level and that radiation-induced blocking of the cell cycle has only a small effect on the expansion several hundred days after the administration of radiation. The resulting model was fitted to dose-response curves for Harderian-gland-tumor prevalence in mice near 600 days in age. The cross sections for inactivation and the mutation associated with the initiation event determined from our fits are of the same order of magnitude as those observed in many experiments with cell culture. For high-energy protons and alpha particles, the addition of the effects of the target fragments produced in nuclear reaction accounted for the increase in tumorigenic potential seen at low dose as compared with  $\gamma$ -rays. The large differences seen in the experiments between protons and alpha particles at high dose could not be explained in our model.

An enhancement in onconogenic effect following protracted exposures to high-linear-energy-transfer (LET) radiation has been observed in many studies in animals and cell culture. By using our approach, we have considered several factors that could lead to such an effect, including cell killing, repopulation, and radiation-induced promotion of initiated cells. The effects of repopulation were seen to lead to an enhancement for a small number of fractions for relativistic iron nuclei; however, for a large number of fractions, the enhancement was not seen because of insufficient time for expansion of initiated cells. The addition of a second mutation induced by

radiation associated with the promotion of initiated cells also leads to an inverse dose-rate effect in the present model. The enhancement using this assumption would be very large if the action cross section for the second mutation was about the same as that of the first mutation, or it would be more modest if the cross section was close to the observed mutation rates in mammalian cells for the HGPRT locus. In all cases considered, the effects of  $\gamma$ -rays are reduced through dose fractionation. In contrast, an inverse dose-rate effect is seen for high-energy protons when radiation is assumed to act as a promoter because of the high-LET component of their effect from nuclear reactions. This effect could have important consequences for space radiation protection.

## Acknowledgement

We thank Michael Fry and Leif Peterson for helpful discussions and Patricia Powers-Risius for providing preprints of their data before publication.

NASA Langley Research Center  
Hampton, VA 23681-0001  
September 15, 1994

## References

- Ainsworth, E. J. 1980: Life Span Studies on Mice Exposed to Heavy Charged Particles or Photons: Preliminary Results. *Biological and Medical Research With Accelerated Heavy Ions at the Bevalac—1977–1980*, M. C. Pirruccello and C. A. Tobias, eds., LBL-11220, (Contract W-7405-ENG-48), Univ. California, pp. 293–301.
- Alpen, E. L.; Powers-Risius, P.; Curtis, S. B.; and DeGuzman, R. 1993: Tumorigenic Potential of High-Z, High-LET Charged-Particle Radiations. *Radiat. Res.*, vol. 136, pp. 382–391.
- Alpen, E. L.; Powers-Risius, P.; Curtis, S. B.; DeGuzman, R.; and Fry, R. J. M. 1994: Fluence-Based Relative Biological Effectiveness for Charged Particle Carcinogenesis in Mouse Harderian Gland. *Advances in Space Research*, Volume 13, pp. 573–582.
- Brenner, D. J.; and Hall, E. J. 1990: The Inverse Dose-Rate Effect for Oncogenic Transformation by Neutrons and Charged Particles: A Plausible Interpretation Consistent With Published Data. *Internat. J. Radiat. Biol.*, vol. 58, no. 5, pp. 745–758.
- Burns, F. J.; and Albert, R. E. 1980: Dose Response for Rat Skin Tumors Induced by Single and Split Doses of Argon Ions. *Biological and Medical Research With Accelerated Heavy Ions at the Bevalac—1977–1980*, M. C. Pirruccello and C. A. Tobias, eds., LBL-11220, (Contract W-7405-ENG-48), Univ. California, pp. 233–235.
- Butts, J. J.; and Katz, Robert 1967: Theory of RBE for Heavy Ion Bombardment of Dry Enzymes and Viruses. *Radiat. Res.*, vol. 30, no. 4, pp. 855–871.

- Chunxiang, Zhang; Dunn, D. E.; and Katz, R. 1985: Radial Distribution of Dose and Cross-Sections for the Inactivation of Dry Enzymes and Viruses. *Radiat. Prot. Dosim.*, vol. 13, nos. 1-4, pp. 215-218.
- Cucinotta, Francis A.; Katz, Robert; Wilson, John W.; Townsend, Lawrence W.; Shinn, Judy L.; and Hajnal, Ferenc 1991: Biological Effectiveness of High-Energy Protons—Target Fragmentation. *Radiat. Res.*, vol. 127, pp. 130-137.
- Dertinger, Hermann; and Jung, Horst (R. P. O. Hüber and P. A. Gresham, transl.) 1970: *Molecular Radiation Biology*. Springer-Verlag.
- Dienes, G. J. 1966: A Kinetic Model of Biological Radiation Response. *Radiat. Res.*, vol. 28, pp. 183-202.
- Di Majo, Vincenzo; Coppola, Mario; Rebessi, Simonetta; Bassani, Bruno; Alati, Teresa; Saran, Anna; Bangrazi, Caterina; and Covelli, Vincenzo 1986: Dose-Response Relationship of Radiation-Induced Harderian Gland Tumors and Myeloid Leukemia of the CBA/Cne Mouse. *JNCI*, vol. 76, no. 5, pp. 955-966.
- Fry, R. J. M. 1981: Experimental Radiation Carcinogenesis: What Have We Learned? *Radiat. Res.*, vol. 87, pp. 224-239.
- Fry, R. J. M.; Powers-Risius, P.; Alpen, E. L.; and Ainsworth, E. J. 1985: High-LET Radiation Carcinogenesis. *Radiat. Res.*, vol. 104, pp. S188-S195.
- Fry, R. J. M.; and Storer, J. B. 1987: External Radiation Carcinogenesis. *Advances in Radiation Biology*, Volume 13, John T. Lett, ed., Academic Press, Inc., pp. 31-91.
- Grahn, Douglas; Lombard, Louise S.; and Cranes, Bruce A. 1992: The Comparative Tumorigenic Effects of Fission Neutrons and Cobalt-60  $\gamma$  Rays in the B6CF<sub>1</sub> Mouse. *Radiat. Res.*, vol. 129, no. 1, pp. 19-36.
- Hill, C. K.; Buonaguro, F. M.; Myers, C. P.; Han, A.; and Elkind, M. M. 1982: Fission-Spectrum Neutrons at Reduced Dose Rates Enhance Neoplastic Transformation. *Nature*, vol. 298, pp. 67-69.
- Katz, R.; Ackerson, B.; Homayoonfar, M.; and Sharma, S. C. 1971: Inactivation of Cells by Heavy Ion Bombardment. *Radiat. Res.*, vol. 47, pp. 402-425.
- Katz, R.; Dunn, D. E.; and Sinclair, G. L. 1985: Thindown in Radiobiology. *Radiat. Prot. Dosim.*, vol. 13, nos. 1-4, pp. 281-284.
- Kranert, T.; Schneider, E.; and Kiefer, J. 1990: Mutation Induction in V79 Chinese Hamster Cells by Very Heavy Ions. *Internat. J. Radiat. Biol.*, vol. 58, no. 6, pp. 975-988.
- Kronenberg, A.; and Little, J. B. 1989: Locus Specificity for Mutation Induction in Human Cells Exposed to Accelerated Heavy Ions. *Internat. J. Radiat. Biol.*, vol. 55, no. 6, pp. 913-924.
- Land, Hartmut; Parada, Luis F.; and Weinberg, Robert A. 1983: Cellular Oncogenes and Multistep Carcinogenesis. *Science*, vol. 222, pp. 771-778.
- Lett, J. T.; Cox, A. B.; Story, M. D.; Ehmann, U. K.; and Blakely, E. A. 1989: Responses of Synchronous L5178Y S/S Cells to Heavy Ions and Their Significance for Radiobiological Theory. *Proc. R. Soc. London*, vol. B 237, pp. 27-42.
- Marshall, John H.; and Groer, Peter G. 1977: A Theory of the Induction of Bone Cancer by Alpha Radiation. *Radiat. Res.*, vol. 71, pp. 149-192.
- Miller, Richard C.; Brenner, David J.; Randers-Pehrson, Gerhard; Marino, Stephen A.; and Hall, Eric J. 1990: The Effects of the Temporal Distribution of Dose on Oncogenic Transformation by Neutrons and Charged Particles of Intermediate LET. *Radiat. Res.*, vol. 124, pp. S62-S68.
- Mitchel, R. E. J.; and Trivedi, A. 1993: Radiation: What Determines the Risk? *Biological Effects and Physics of Solar and Galactic Cosmic Radiation, Part B*, Charles E. Swenberg, Gerda Horneck, and E. G. Stassinopoulos, eds., Plenum Press, pp. 859-870.
- Moolgavkar, Suresh H.; and Knudson, Alfred G., Jr. 1981: Mutation and Cancer: A Model for Human Carcinogenesis. *JNCI*, vol. 66, no. 6, June, pp. 1037-1051.
- Moolgavkar, Suresh H.; Cross, Fredrick T.; Luebeck, Georg; and Dagle, Gerald E. 1990: A Two-Mutation Model for Radon-Induced Lung Tumors in Rats. *Radiat. Res.*, vol. 121, pp. 28-37.
- National Council on Radiation Protection Measurements. The Relative Biological Effectiveness of Radiations of Different Quality. NCRP No. 104, Dec. 1990.
- Nelson, Gregory A.; Schubert, Wayne W.; Marshall, Tamara M.; Benton, Eric R.; and Benton, Eugene V. 1989: Radiation Effects in *Caenorhabditis Elegans*, Mutagenesis by High and Low LET Ionizing Radiation. *Mutation Res.*, vol. 212, pp. 181-192.
- Renan, Michael J. 1990: Cancer Genes: Current Status, Future Prospects, and Applications in Radiotherapy/Oncology. *Radiother. & Oncology*, vol. 19, no. 3, pp. 197-218.
- Thacker, John; Stretch, Albert; and Stephens, Miriam A. 1979: Mutation and Inactivation of Cultured Mammalian Cells Exposed to Beams of Accelerated Heavy Ions. II. Chinese Hamster V79 Cells. *Int. J. Biol.*, vol. 36, no. 2, pp. 137-148.
- Tsuboi, Koji; Yang, Tracy C.; and Chen, David J. 1992: Charged-Particle Mutagenesis. I. Cytotoxic and Mutagenic Effects of High-LET Charged Iron Particles on Human Skin Fibroblasts. *Radiat. Res.*, vol. 129, no. 2, pp. 171-176.
- Ullrich, R. L.; Jernigan, M. C.; and Storer, J. B. 1977: Neutron Carcinogenesis—Dose and Dose-Rate Effects in BALB/c Mice. *Radiat. Res.*, vol. 72, pp. 487-498.
- Ullrich, R. L. 1984: Tumor Induction in BALB/c Mice After Fractionated or Protracted Exposures to Fission-Spectrum Neutrons. *Radiat. Res.*, vol. 97, pp. 587-597.

Upton, A. C. 1986: Dose-Incidence Relations for Radiation Carcinogenesis With Particular Reference to the Effects of High-LET Radiation. *Radiation Carcinogenesis and DNA Alterations*, F. J. Burns, A. C. Upton, and G. Silini, eds., Plenum Press, pp. 115–137.

Wilson, John W.; Cucinotta, F. A.; and Shinn, J. L. 1993: Cell Kinetics and Track Structure. *Biological Effects*

*and Physics of Solar and Galactic Cosmic Radiation, Part A*, C. E. Swenberg, Gerda Horneck, and E. G. Stassinopoulos, eds., Plenum Press.

Yang, Tracy Chui-Hsu; Craise, Laurie M.; Mei, Man-Tong; and Tobias, Cornelius A. 1985: Neoplastic Cell Transformation by Heavy Charged Particles. *Radiat. Res.*, vol. 104, pp. S177–S187.

REPORT DOCUMENTATION PAGE			Form Approved OMB No. 0704-0188	
Public reporting burden for this collection of information is estimated to average 1 hour per response, including the time for reviewing instructions, searching existing data sources, gathering and maintaining the data needed, and completing and reviewing the collection of information. Send comments regarding this burden estimate or any other aspect of this collection of information, including suggestions for reducing this burden, to Washington Headquarters Services, Directorate for Information Operations and Reports, 1215 Jefferson Davis Highway, Suite 1204, Arlington, VA 22202-4302, and to the Office of Management and Budget, Paperwork Reduction Project (0704-0188), Washington, DC 20503.				
1. AGENCY USE ONLY (Leave blank)	2. REPORT DATE December 1994	3. REPORT TYPE AND DATES COVERED Technical Paper		
4. TITLE AND SUBTITLE Kinetics Model for Initiation and Promotion for Describing Tumor Prevalence From HZE Radiation			5. FUNDING NUMBERS WU 199-45-16-11	
6. AUTHOR(S) Francis A. Cucinotta and John W. Wilson				
7. PERFORMING ORGANIZATION NAME(S) AND ADDRESS(ES) NASA Langley Research Center Hampton, VA 23681-0001			8. PERFORMING ORGANIZATION REPORT NUMBER L-17404	
9. SPONSORING/MONITORING AGENCY NAME(S) AND ADDRESS(ES) National Aeronautics and Space Administration Washington, DC 20546-0001			10. SPONSORING/MONITORING AGENCY REPORT NUMBER NASA TP-3479	
11. SUPPLEMENTARY NOTES				
12a. DISTRIBUTION/AVAILABILITY STATEMENT  Unclassified-Unlimited Subject Category 52 Availability: NASA CASI (301) 621-0390			12b. DISTRIBUTION CODE	
13. ABSTRACT (Maximum 200 words) A kinetics model for cellular repair and misrepair for multiple radiation-induced lesions (mutation-inactivation) is coupled to a two-mutation model of initiation and promotion in tissue to provide a parametric description of tumor prevalence in the Harderian gland in a mouse. Dose-response curves are described for $\gamma$ -rays and relativistic ions. The effects of nuclear fragmentation are also considered for high-energy proton and alpha-particle exposures. The model described provides a parametric description of age-dependent cancer induction for a wide range of radiation fields. We also consider the two hypotheses that radiation acts either solely as an initiator or as both initiator and promoter and make model calculations for fractionation exposures from $\gamma$ -rays and relativistic Fe ions. For fractionated Fe exposures, an inverse dose-rate effect is provided by a promotion hypothesis using a mutation rate for promotion typical of single-gene mutations.				
14. SUBJECT TERMS Radiation carcinogenesis; Galactic cosmic rays; Initiation-promotion models			15. NUMBER OF PAGES 17	
			16. PRICE CODE A03	
17. SECURITY CLASSIFICATION OF REPORT Unclassified	18. SECURITY CLASSIFICATION OF THIS PAGE Unclassified	19. SECURITY CLASSIFICATION OF ABSTRACT Unclassified	20. LIMITATION OF ABSTRACT	